# Towards centimeter accurate positioning with smartphones

**Anja Heßelbarth, Lambert Wanninger**

Geodetic Institute, Technical University Dresden
Dresden, GERMANY
email: anja_brit.hesselbarth@tu-dresden.de

**Associated ENC 2020 topic:** B: GNSS Algorithms & Techniques, high-accurately positioning w./o. augmentation services

***Abstract:***

*Nowadays, Android enables the access of GNSS raw data and, thus, an in-depth evaluation of smartphone GNSS observations. We analysed and compared GNSS code and phase observations and the achievable position accuracies of three Android devices: tablet Google Nexus 9, smartphones Xiaomi Mi8 and Huawei P30. Not all the phase observables of these devices possess the property of integer ambiguities. We were able to perform precise antenna calibrations on GPS L1 for both smartphones and obtained corrections for the phase center offsets and phase center variations. The latter do not exceed 1 to 2 cm. With successful ambiguity fixing, we achieved standard deviations of the 3D positions of 2 to 3 cm after 30 minutes of static observations in baseline mode.*

## 1 Introduction

Since the introduction of Android 7 (Nougat) in 2016, GNSS observations of mobile devices like smartphones or tablets can be processed or stored in files by Android Apps, which allows data analysis and position estimation in post-processing [1],[2]. Thus, new or extended areas of applications for positioning with smartphones and tablets become feasible. One of the challenges is to improve positioning accuracy to centimeter level. This requires processing of the carrier phase observations and the fixing of their integer ambiguities.
One of the first Android devices with the capability to receive and record phase observations is Google Nexus 9 tablet. This tablet embeds a Broadcom BCM4752 GNSS receiver, capable of tracking GPS, GLONASS and QZSS, but only on the first frequency [3],[4]. Since 2018, smartphones have been offered which track GNSS code and phase on two frequencies. The second frequency increases signal availability, enables ionosphere monitoring, and ambiguity fixing is simplified by using a widelane linear combination. The first dual-frequency mass-market GNSS chip was BCM47755 Chip which is embedded in Xiaomi Mi8 (May 2018). In August 2018, the announcement of the Kirin 980 chipset followed which is integrated in Huawei P30 [5].
In the last 3 years many researchers investigated the position accuracies by using smartphone observations. However, the achievable accuracies depend on the positioning algorithm. Often the results are obtained in absolute mode without carrier phase ambiguity fixing and achieve m up to dm accuracies [6], [7], [8]. First results based on baseline processing with carrier phase ambiguity fixing demonstrated that cm-accuracy is feasible [9], [10].
In this work we present our experiences with GNSS observations by Nexus 9 tablet, and the smartphones Xiaomi Mi8 and Huawei P30. We analysed the data with respect to the availability of the GNSS observations and the quality of code and phase. Furthermore, we investigated

whether the carrier phase observations possess the property of integer ambiguities and calibrated the internal GNSS antennas. At the end, we calculated static baselines with respect to a nearby reference station using various processing methods.

## 2 Data collection and availability

We designed and built holders for the tablet and the smartphones to enable measurements in an upright position and to mount the devices on tribrach or tripod. All measurements were performed in the same roof top environment where no obstructions could disturb the signals (Figure 1). On the same roof top, we also operated a reference station equipped with a Septentrio PolaRx5 receiver and a Jav RingAnt_DM JVDM antenna.
GNSS observations were performed with the Nexus 9 in March/April 2017, with the Huawei P30 in June/July 2019, and with the Xiaomi Mi8 at the end of 2019 and in early 2020. We tried to collect long observation sessions, however the data recording usually ended after several (6) or many (18) hours. We were not able to identify the causes for these early terminations of the data recordings.

Figure 1: Mobile devices on a tribrach. Left: Google Nexus 9 with weather protection. Middle: Huawei P30 with defined north orientation. Right: Xiaomi Mi8 with defined north orientation.

GNSS observation were written to ASCII output files by using the Android App GNSS Logger [1], [11]. We wrote a converter to store code, phase and doppler measurements as well as signal strengths in Receiver Independent Exchange Format (RINEX) [12]. The data analysis and evaluation were realized with tools of the GNSS post-processing software WaSoft, developed by the second author.
The BCM4752 chip embedded in the Nexus 9 collects data from GPS, GLONASS, QZSS on the 1st frequency only [13]. The chip-manufactures of the phones, see [14] and [15], specify that the GNSS chips are able to track signals of GPS and Galileo on frequency 1 and 5, BeiDou and GLONASS on the 1st frequency. QZSS is tracked on its 1st frequency (Xiaomi Mi8) or on frequencies 1 and 5 (Huawei P30).
Table 1 gives an overview of the received observation data. It is recognizable that not all available GNSS signals could be recorded. This mainly concerns Galileo and BeiDou observations tracked by the Xiaomi Mi8. With this device, we could only track Galileo or BeiDou satellites which were available when starting the device or GNSS app. Satellites which became visible later on could not be recorded. After some hours all these satellites had set and no Galileo or BeiDou observations were performed until these earlier satellites reappeared. Another peculiarity concerns the Huawei P30: GLONASS signal with frequency channel numbers -7 and 6 were not tracked.

Table 1: Average number of signals tracked on stations without any signal obstructions (recorded by GNSSLogger)

| GNSS | Nexus 9 (2017) | Xiaomi Mi8 (2019/20) | Huawei P30 (2019) |
|---|---|---|---|
| **GPS** | L1: 7.5 | L1: 11.0; L5: 4.0 | L1: 10.0; L5: 4.0 |
| **Galileo** | - | E1: 3.5; E5a: 3.5 | E1: 4.5; E5a: 5.5 |
| **GLONASS** | R1: 6.0 | R1: 7.0 | R1: 7.0 |
| **BeiDou** | | B1-2: 4,0 | B1-2: 5.5 |

## 3 Signal strength and quality

GNSS observation data sets are accompanied by signal strength measurements in form of a carrier-to-noise power density ratio ($C/N_0$) in dB-Hz. This information enables an evaluation of the observation qualities as well as antenna gains as a function of the signal's incidence angles.

Figure 2 shows the $C/N_0$ values as a function of elevation angle for all available GNSS signals of Nexus 9, Xiaomi Mi8, and Huawei P30 and, for comparison, of a geodetic-grade equipment (receiver: Septentrio PolaRx5, antenna: NavX3G+C).

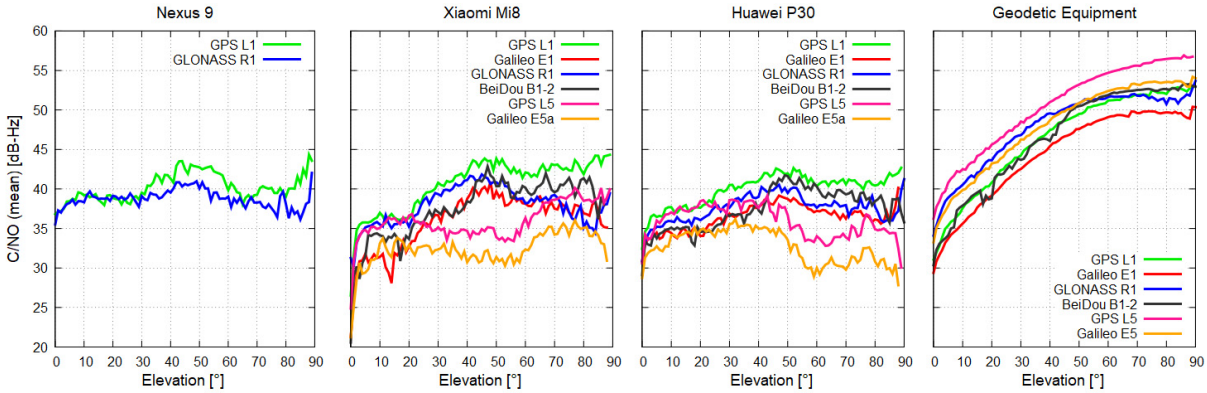


Figure 2: Elevation-dependent $C/N_0$ of the GNSS observations of Google Nexus N9, Xiaomi Mi8, Huawei P30, and geodetic-grade equipment

Figure 2 confirms earlier findings of, e.g. [5],[6],[16] that $C/N_0$ values for the mobile devices are on average 10 dB-Hz lower as compared to geodetic-grade equipment. The GNSS signal-to-noise values of the mobile devices vary only little with incidence angle, whereas $C/N_0$ values of geodetic antennas show a typical elevation-dependent behaviour, see [5],[6],[16],[17]. Another characteristic of these smartphone antennas is, that they are more sensitive to L1/E1/R1/B1-2 signals as compared to L5/E5a.

The quality of code measurements can be assessed from the comparison with phase measurements. This method uses the so called multipath linear combination [18], also called code-minus-carrier combination [19]. If dual-frequency data exists, the combination is free from ionospheric or tropospheric effects as well as from inaccurate or unknown satellite or receiving antenna positions. It is mainly affected by multipath and noise. Since we obtained our measurements on a roof top, we have no signal obstructions and a low level of signal reflections.

Figure 3 presents elevation-dependent RMS values of the multipath linear combination (MP) for all signals. Table 2 contains MP RMS values for the whole elevation range. Nexus 9 exhibits

MP values of 3 to 4 m, the largest in this group of equipment. The two smartphones show MP values for signals on the 1st frequency of around 2 meters. The MP values of the L5/E5a signals of Xiaomi Mi8 are smaller by a factor of 2 and, therefore, promise higher accuracy for code-based positioning methods. However, the number of satellites with L5/E5a signals is still much smaller than the number of satellites with L1/E1 signals.

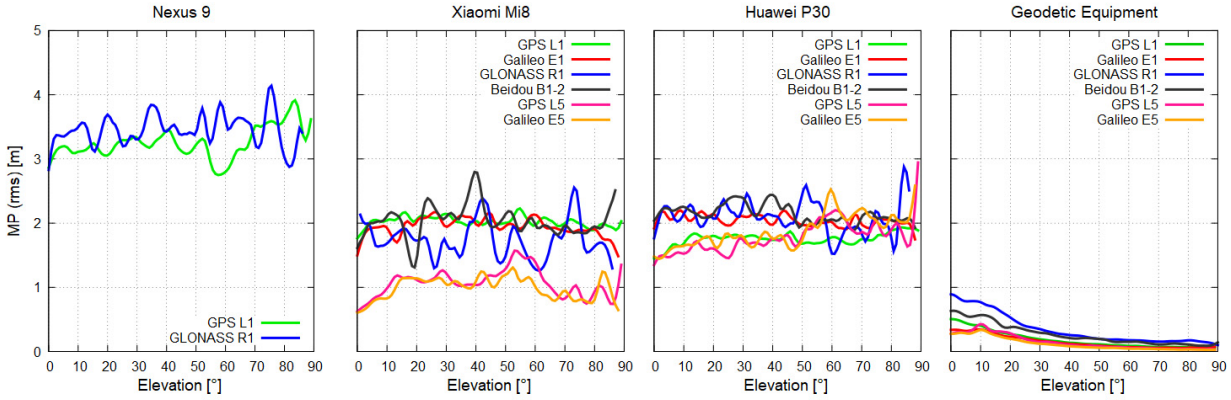


Figure 3: Elevation-dependent MP of GNSS observations of Google Nexus 9, Xiaomi Mi8, Huawei P30, and geodetic-grade equipment

The MP values of the mobile devices do not show much of an elevation-dependence. The geodetic equipment exibits a strong elevation-dependence of MP, but on the much lower level of a few decimeters.

Table 2: RMS of code residuals from code-carrier differences over the whole elevtion angle range

| **GNSS** | **Quality of code observation [m]** | | | |
|---|---|---|---|---|
| | **Nexus 9** | **Xiaomi Mi8** | **Huawei P30** | **Geodetic equipment** |
| **GPS** | L1: 3.0 | L1: 2.0; L5: 1.1 | L1: 1.8; L5: 1.8 | L1: 0.2; L5: 0.2 |
| **GALILEO** | - | E1: 2.0; E5: 1.0 | E1: 2.0; E5: 1.8 | E1: 0.2; E5: 0.1 |
| **GLONASS** | R1: 3.2 | R1: 2.0 | R1: 2.2 | R1: 0.4 |
| **BeiDou** | - | B1-2: 1.9 | B1-2: 2.1 | B1-2: 0.3 |

## 4 Ambiguity fixing rate

Prerequisite for a successful ambiguity fixing is that the carrier phase ambiguities possess integer property. In order to verify this property, we calculated double difference (DD) residuals in a short and known baseline to a GNSS reference station. Due to the baseline length of just a few meters, the DD residuals are free from atmospheric effects and not influenced by orbit errors. They contain carrier phase multipath, noise and maybe differential instrumental delays, which can prevent the integer property of the ambiguities [9].

Figure 4 illustrates the distribution of fractional DD residuals for all available GNSS observations of the 3 mobile devices and the geodetic equipment. A pronounced maximum around zero cycles indicates the property of integer ambiguities.

The fractional DD residuals based on observations of Nexus 9 reveal no maximum and, thus, ambiguity fixing cannot be performed successfully. In contrast, the fractional DD residuals of the Xiaomi Mi8 exhibit clear maxima for GPS L1 and L5, for Galileo E1 and E5a, and for BeiDou B1-2. Around 50 % of all fractional DD residuals fall into the interval from -0.1 to +0.1

cycles. No similar maximum can be seen for GLONASS G1. The Huawei P30 fractional DD residuals reveal just one signal with the property of integer ambiguities: GPS L1. As expected, the geodetic equipment exhibits pronounced maxima on all signals. Usually, more than 90 % of all fractional DD residuals fall into the interval from -0.1 to +0.1 cycles.

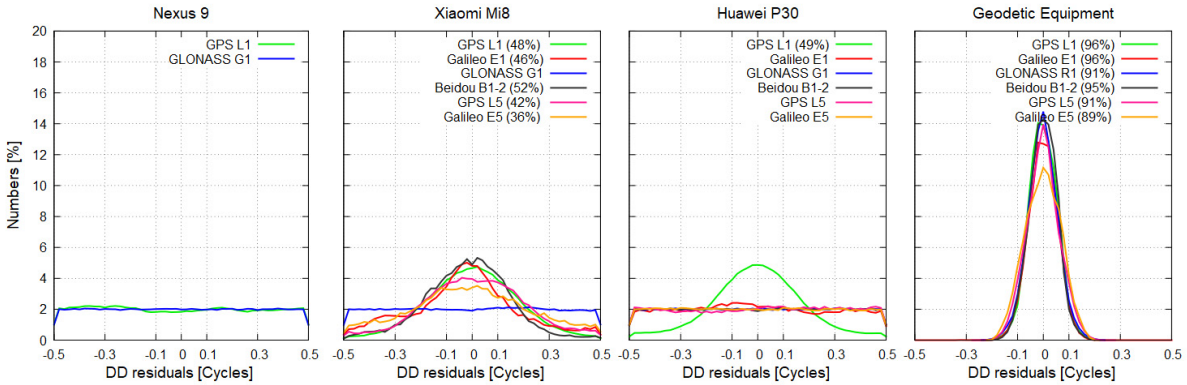


Figure 4: Distribution of fractional double difference residuals of Google Nexus N9, Xiaomi Mi8, Huawei P30, and the geodetic-grade equipment; the short and knwon baselines were formed with respect to a geodetic GNSS reference station; the percentages given in parentheses refer to the range of -0.1 to +0.1cycles

# 5 Calibration of smartphone antennas

Precise information about the phase center offset (PCO) and phase center variations (PCV) are required to achieve cm-accurate positioning results. An accurate calibration can only be performed if the integer carrier phase ambiguities could be fixed and a large number of observations is available. For these two reasons, we could only successfully calibrate the Xiaomi Mi8 in combination of GPS L1/Galileo E1 and the Huawei P30 on GPS L1.

We defined the antenna reference point (ARP) to be in the center of the lower edge of the smartphone in upright position. We defined north direction to be the azimuthal orientation where the display is pointing south [9]. We used the calibration method where the local reference station is fixed and the observations of the antenna to be calibrated are performed in four azimuthal directions (0°, 90°, 180°, 270°). The geodetic reference station was equipped with a calibrated JavRingAnt_DM JVDM antenna. Since the baseline between smartphones and reference station was shorter than 10 m, the calibration results are not affected by atmospheric effects and orbit errors.

The calibration was realized in two different ways. In the manual mode we observed four sessions (> 6h) with different azimuthal orientations. In the automatic mode we used a rotation device which rotates the antenna to the four different azimuthal orientations every minute [20] and records one session (>6h). Based on this observation data and the levelled height difference between reference antenna and antenna to be calibrated, we estimated three dimensional PCO and PCV for the complete upper hemisphere.

The two independent calibration results for each antenna agree on the 1-2 cm level for the Huawei P30 and on the 1 cm level for the Xiaomi Mi8. We combined the pairs of calibration results to obtain our final PCO and PCV corrections (Figure 5).

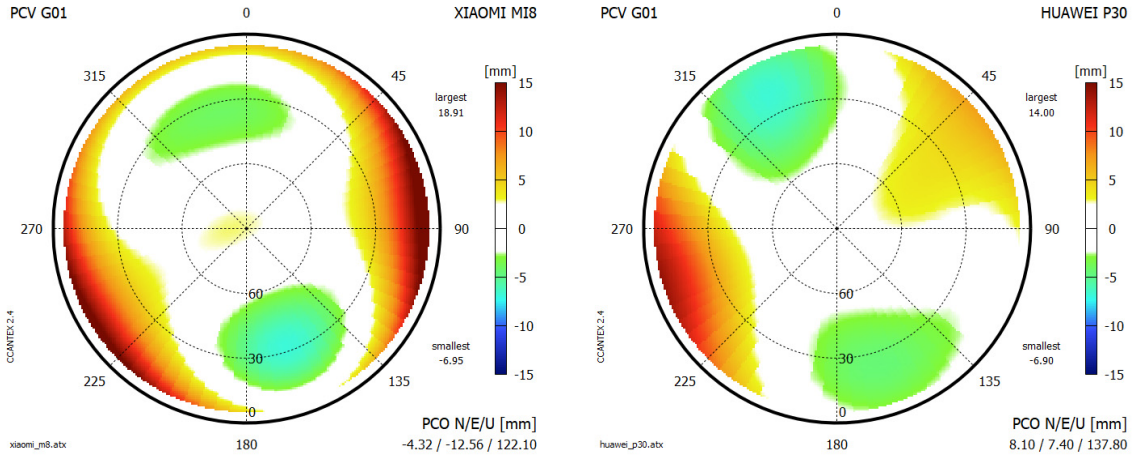


Figure 5: GPS L1 / Galileo E1 phase center variations and phase center offsets for Xiaomi Mi8 and Huawei P30

The PCVs correction values range between -5 and +15 mm and both antennas reveal a similar pattern. The PCO height values indicate that the antennas are located near the upper edges of the smartphones in upright position. The east components have different signs. This means that the PCO of Huawei P30 is located more to the right and of Xiaomi Mi8 more to the left.

# 6 Accuracy of positioning based on smartphone observations

To analyse the achievable positioning accuracy, we divided our observation sessions into blocks of 5 to 120 minutes. We determined the baseline vector between the geodetic reference station and the mobile devices. After some modifications of the processing engine, like the adjustment of the thresholds for outlier detection and ambiguity fixing, and the observation weighting, we obtained three kinds of baseline solutions:

- code-differential (DGNSS),
- carrier phase differential without ambiguity fixing (“float”),
- carrier phase differential with ambiguity fixing (“fixed”).

All results are based on code and phase observations of GPS L1 only. There are no “fixed”-solutions for the Nexus 9 due to the inability to fix the phase ambiguities to integers. We compared the positioning results with the known baseline vectors and calculated 3D deviations (Figure 6).

The DGNSS deviations are on the 1 to few meter level, the float deviations are one order of magnitude smaller. The convergence of the positioning solutions can be seen best with the “float”-solutions: with 5 minutes of observations the 3D deviations amount to approximately 1 m and after 90 minutes the differences are smaller than one decimeter for the two smartphones. The “fixed”-solutions achieve a 3D RMS of few centimeters if the ambiguities could be fixed successfully. This clearly demonstrates that cm-accurate positioning is achievable with smartphone GNSS observations.

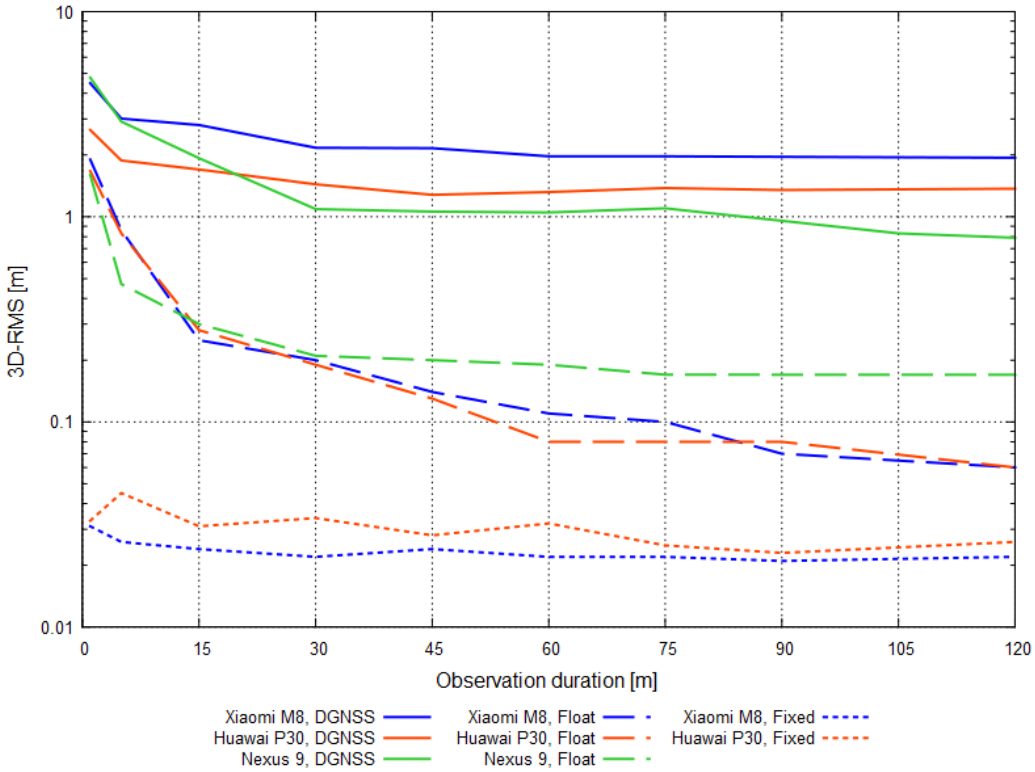


Figure 6: Accuracy of different processing methods for observations based on Xiaomi M8, Huawei P30 and Nexus 9

## 7 Conclusions

We analysed the GNSS observations of three different Android mobile devices which are capable to provide carrier phase observations. Unfortunately, not all carrier phase observations have the property of integer ambiguities. But cm-accurate positioning can only be achieved if the ambiguities are fixed to their correct integer values.
Ambiguity fixing is also necessary for the calibration of the antenna phase centers. We determined phase center offsets and variations for GPS L1 / Galileo E1 and applied them as corrections in the position calculation.
We could demonstrate that cm-accurate positioning is possible with carrier phase observations after successful ambiguity fixing.

## Acknowledgments

The authors are grateful to Lisa Salzmann and Danielle Warstat for collecting most of the Xiaomi Mi8 and Huawei P30 observation data and to Volker Frevert for his support of the phase center calibration.

## References

[1] S. Banville and F. v Diggelen, “Precise GNSS for Everyone: Precise Positioning Using Raw GPS Measurements,” *GPS World*, 2016, vol. 27, pp. 43–48.
[2] GSA, “Using GNSS Raw Measurements on Android Devices: Towards better location performance in mass market application,” 2017, doi: 10.2878/449581.

[3] M. Håkansson, “Characterization of GNSS observations from a Nexus 9 Android tablet,” *GPS Solut*, 2019, vol. 23, no. 1, p. 43, doi: 10.1007/s10291-018-0818-7.
[4] E. Realini, S. Caldera, L. Pertusini, and D. Sampietro, “Precise GNSS Positioning Using Smart Devices,” *Sensors*, 2017, vol. 17, no. 10, p. 2434, doi: 10.3390/s17102434.
[5] L. Massarweh, F. Darugna, D. Psychas, and J. Bruno, “Statistical Investigation of Android GNSS Data: Case Study Using Xiaomi Mi 8 Dual-Frequency Raw Measurements,” *Proceedings of the 30th International Technical Meeting of the Satellite Division of The Institute of Navigation, Miami, Florida*, 2019, 2019.
[6] A. Elmezayen and A. El-Rabbany, “Precise Point Positioning Using World's First Dual-Frequency GPS/GALILEO Smartphone,” *Sensors (Basel, Switzerland)*, vol. 2019, no. 11, doi: 10.3390/s19112593.
[7] Q. Wu, M. Sun, C. Zhou, and P. Zhang, “Precise Point Positioning Using Dual-Frequency GNSS Observations on Smartphone,” *Sensors (Basel, Switzerland)*, 2019, vol. 19, no. 9, doi: 10.3390/s19092189.
[8] D. Laurichesse, C. Rouch, F. Marmet, R. Francois-Xavier, and M. Pascaud, “Smartphone Applications for Precise Point Positioning,” *Proceedings of the 30th International Technical Meeting of the Satellite Division of The Institute of Navigation, Portland, Oregon*, vol. 2017, doi: 10.33012/2017.15149.
[9] L. Wanninger and A. Heßelbarth, “GNSS code and carrier phase observations of a Huawei P30 smartphone: Quality assessment and centimeter-accurate positioning,” *GPS Solut*, 2020, vol. 24, no. 2, p. 43, doi: 10.1007/s10291-020-00978-z.
[10] F. Darugna, J. Wübbena, A. Ito, T. Wübbena, G. Wübbena, and M. Schmitz, “RTK and PPP-RTK Using Smartphones: From Short-Baseline to Long-Baseline Applications,” *Proceedings of the 30th International Technical Meeting of the Satellite Division of The Institute of Navigation, Miami, Florida*, vol. 2019, doi: 10.33012/2019.17078.
[11] F. van Diggelen, F. and M. Khider, “GNSS Analysis Tools from Google.,” *Inside GNSS*, vol. 2018, pp. 48–57. https://insidegnss.com/gnss-analysis-tools-from-google/
[12] IGS/RTCM, *RINEX The Receiver Independent Exchange Format: version 3.04*. 2018. ftp://igs.org/pub/data/format/rinex303.pdf
[13] Broadcom, *Integrated Multi-Constellation GNSS Receiver*. 2017. https://www.broadcom.com/products/wireless/gnss-gps-socs/bcm4752
[14] Huawei P30, *Huawei P30 - specifications*. 2017. https://consumer.huawei.com/en/phones/p30/specs/
[15] Broadcom, *BCM4775X-GNSS Receiver with Integrated Sensor Hub: Productbrief*. 2017. https://www.broadcom.cn/products/wireless/gnss-gps-socs/bcm47755
[16] X. Zhang, X. Tao, F. Zhu, X. Shi, and F. Wang, “Quality assessment of GNSS observations from an Android N smartphone and positioning performance analysis using time-differenced filtering approach,” *GPS Solut*, 2018, vol. 22, no. 3, p. 21, doi: 10.1007/s10291-018-0736-8.
[17] J. Paziewski, “Recent advances and perspectives for positioning and applications with smartphone GNSS observations,” *Meas. Sci. Technol.*, 2020, vol. 31, no. 9, p. 91001, doi: 10.1088/1361-6501/ab8a7d.
[18] M. Braasch, “Multipath,” *In: Teunissen P.J.G., Montenbruck, O. Springer handbook of global navigation satellite systems*, 2017, pp. 443–468.
[19] A. Hauschild, “Combination of Observations,” *In: Teunissen P.J.G., Montenbruck, O. Springer handbook of global navigation satellite systems*, 2017, pp. 586–604.
[20] A. Schmolke, L. Wanninger, V. Frevert, “Erste GNSS-Antennenkalibrierungen im Feldverfahren auf neuen Signalfrequenzen,” *ZfV-Zeitschrift für Geodäsie, Geoinformation und Landmanagement*, vol. 2015, pp. 283–289.